Proc. Natl. Acad. Sci. USA
Vol. 95, pp. 2486–2491, March 1998
Immunology

Two distinct pathways of positive selection for thymocytes

KOICHI AKASHI*, MOTONARI KONDO, AND IRVING L. WEISSMAN

Departments of Pathology and Developmental Biology, Stanford University School of Medicine, Stanford, CA 94305

Contributed by Irving L. Weissman, December 16, 1997

ABSTRACT **Most mouse thymocytes undergoing positive selection are found on one of two pathways; the c-Kit$^+$ and the c-Kit$^-$ pathways. Here, we show that c-Kit and interleukin-7 receptor (IL-7R)-mediated signals support positive selection during the transition from the subpopulation that first expresses cell surface T cell receptor (TCR)—the TCRα/β^{lo}CD4^{int}/CD8^{int} (DP^{int}) c-Kit$^+$ cells to TCRα/β^{med}c-Kit$^+$ transitional intermediate cells (the c-Kit$^+$ pathway). Cells that fail positive selection on the c-Kit$^+$ pathway become TCRα/β^{lo}c-Kit$^-$ (DP^{hi}) blasts that appear to undergo alternative TCRα rearrangements. The rare DP^{hi}c-Kit$^-$ blast cells that thus are salvaged for positive selection by expressing a self-major histocompatibility complex selectable TCRα/β up-regulate IL-7R, but not c-Kit, and are the principal progenitors on the c-Kit$^-$ pathway; this c-Kit$^-$IL-7R$^+$ pathway is mainly CD4 lineage committed. Cell division is a feature of the TCR$^{lo\text{-}med}$c-Kit$^+$ transition, but is not essential for CD4 lineage maturation from DP^{hi}c-Kit$^-$ blasts. In this view, positive selection on the c-Kit$^-$ path results from a salvage of cells that failed positive selection on the c-Kit$^+$ path.**

The thymus is the major site of differentiation of T lymphocytes. The earliest thymic precursors [such as CD3$^-$4^{lo}8$^-$ (1) or the CD3$^-$4$^-$8$^-$ triple negative (TN) cells] that express c-Kit and interleukin-7 receptor (IL-7R) rearrange T cell receptor (TCR) β and α chains, and become TCR^{lo}CD4$^+$8$^+$ (double positive, DP) cells. Both steel factor (Slf) and IL-7 are major factors involved in the expansion of immature thymocytes (2, 3).

DP cells are heterogenous; they include the majority of thymocytes destined to die because of failure in receiving positive selection, as well as cells at the earliest stages of positive selection (4–6). Although the majority of DP cells have shut down IL-7R expression, single positive (SP) cells express IL-7R (7). Recently, we have reported that positively selected TCR^{med}CD69$^+$ thymocytes up-regulate IL-7R, and the IL-7R-mediated signals play a critical role in maintaining survival of the cells at least through up-regulating Bcl-2 (8, 9).

Positive selection can be initiated by two different subsets of the DP fraction: the CD4^{int}CD8^{int} (DP^{int}) TCR^{lo}c-Kit$^+$ cells and the DP^{hi}TCR^{lo}c-Kit$^-$ cells (6). Positive selection of DP^{int} TCR^{lo}c-Kit$^+$ progenitors results in sequential differentiation of TCR$^{med\text{-}hi}$ c-Kit$^+$ transitional intermediates (TIs) that up-regulate CD4 or CD8 (CD4$^+$CD8$^{lo\text{-}med}$ or CD4$^{lo\text{-}med}$CD8$^+$), ending as the TCR^{hi}c-Kit$^-$ (CD4$^+$8$^-$ or CD4$^-$8$^+$) SP cells, without passing through a DP^{hi} stage (the c-Kit$^+$ pathway) (6). The DP^{int}TCR^{lo}c-Kit$^+$ cells generate both CD4 and CD8 SP cells 4 days after intrathymic (i.t.) injection, the ratio of which was ≈2 to 1. When the DP^{int}TCR^{lo} cells fail to receive positive selection, they down-regulate c-Kit and become DP^{hi}TCR^{lo}c-Kit$^-$ blasts (6).

The DP^{hi}TCR^{lo}c-Kit$^-$ blast pool also contains relatively infrequent cells that respond to positive selection. The positive selection of DP^{hi}TCR^{lo} cells does not involve the up-regulation of c-Kit (6, 8). We hypothesized that the c-Kit$^-$ pathway may be a salvage pathway for positive selection of DP^{hi} cells that had failed to receive positive selection at the DP^{int}TCR^{lo}c-Kit$^+$ stage (6), but might be salvaged by rearranging and expressing other TCRα chains (10, 11).

These data raise the possibility of biological and developmental differences during positive selection between the c-Kit$^+$ and c-Kit$^-$ pathways. We delineate these two pathways by evaluating the expression of IL-7R as well as c-Kit, time course, cell cycle status, and contribution to generation of SP progeny.

MATERIALS AND METHODS

Mice. C57BL6/Ka (Ly5.2) and C57BL6 Ly5.1 mice were bred and maintained in the central animal facility in the Department of Comparative Medicine, Stanford University. Mice with H-2^b haplotype (Eα^-) (Ly 5.2) with a targeted mutation in the β2 microglobulin gene [major histocompatibility complex (MHC) class I knockout; MHC-IKO], and a null mutation in the Aβ^b gene (MHC class II knockout; MHC-IIKO) (12) were kindly provided by M. J. Grusby and L. H. Glimcher (Harvard School of Public Health). MHC-class I and II double knockout (MHC-DKO) mice were obtained by intercrossing these mice strains. All of these mice were used between 3 and 5 weeks of age.

Cell Sorting and Analysis. The antibodies used in immunofluorescence staining included AL1–4A2 (anti-Ly5.1); 2B8 (anti-c-Kit, CD117); KT-31 (anti-CD3); H57–579 (anti-TCR-β); GK-1.5 (anti-CD4), and 53–6.7 (anti-CD8). Neutralizing anti-c-Kit (ACK2) and neutralizing anti-IL-7Rα (A7R34) antibodies were kind gifts from S. Nishikawa (Kyoto University, Japan). Because virtually all thymocytes express the common cytokine receptor γ chain, thymocytes that express the IL-7Rα chain should possess a functional IL-7R heterodimer (13). These antibodies were directly conjugated with phycoerythrin (PE), fluorescein-5-isothiocyanate (FITC), allophycocyanin, or Texas Red. A7R34 was biotinylated and visualized by avidin-PE or avidin-Cy5-PE (Becton Dickinson). FITC-conjugated H1.2F3 (anti-CD69) was purchased from PharMingen. The fluorescence was analyzed by using a highly modified dual- or triple-laser FACS. Procedures of i.t. injection and analysis of progeny have been reported elsewhere (4).

PKH26 Labeling of Thymocytes. The details of the PKH analysis have been reported elsewhere (8). Freshly isolated thymocytes were labeled with PKH26 (PKH26 red fluorescent general cell linker kit, Sigma). We measured the first peak of PKH26 signal in the donor-derived (injected) DP fraction (in

The publication costs of this article were defrayed in part by page charge payment. This article must therefore be hereby marked "*advertisement*" in accordance with 18 U.S.C. §1734 solely to indicate this fact.

Abbreviations: IL-7R, interleukin-7 receptor; TCR, T cell receptor; MHC, major histocompatibility complex; DP, double positive; SP, single positive; TI, transitional intermediate; i.t., intrathymic; IKO, class I knockout; IIKO, class II knockout; DKO, double knockout.

*To whom reprint requests should be addressed at: Department of Pathology, B-261 Beckman Center, Stanford, CA 94305. e-mail: Akashi@Darwin.Stanford.edu.

which most cells could not divide) every day after i.t. injection to set a control value of PKH26 (8).

RESULTS

IL-7R Is Expressed in Positively Selected Thymocytes on both c-Kit$^+$ and c-Kit$^-$ Pathways. IL-7R$^+$ cells in normal C57BL6 thymus are represented at all stages of maturation, namely DN, DP^{lo}, DP^{int}, DP^{hi}, TIs, and SP cells (Fig. 1*A*). The IL-7R is expressed in a majority of cells on the c-Kit$^+$ pathway; most TCR^{med} TIs are positive for IL-7R (Table 1). The IL-7R also is expressed in a minority of DP^{hi}c-Kit$^-$ cells (Fig. 1*A*); these DP^{hi}c-Kit$^-$IL-7R$^+$ cells constitute ≈0.2–0.3% of thymocytes and are mainly TCR^{med} (Table 1) and CD69^{med} (data not shown), suggesting that they had just received positive selection signals. The TCR^{med}c-Kit$^-$IL-7R$^+$ TIs in the normal thymus are likely cells differentiating on the c-Kit$^-$ maturation pathway from these DP^{hi}c-Kit$^-$IL-7R$^+$ cells (Table 1).

Mice lacking expression of MHC class I and II by targeted germ-line mutation (MHC-DKO) lack both the c-Kit$^+$ and c-Kit$^-$ maturation pathways, but accumulate the DP^{hi}c-Kit$^-$IL-7R$^-$ cells that are TCR^{lo} to TCR^{med} (Fig. 1 and Table 1). The c-Kit$^+$ population in the MHC-DKO mice are present as the most immature DN/DP^{lo}TCR$^-$ cells (Fig. 1). The DN/DP^{lo}TCR$^-$c-Kit$^+$ cells likely down-regulate c-Kit after failed positive selection to become DP^{hi}TCR$^{lo\text{-}med}$c-Kit$^-$IL-7R$^-$ cells. The MHC-DKO mice did not have either DP^{int}TCR^{lo}c-Kit$^+$IL-7R$^+$ cells, TCR^{med}c-Kit$^+$IL-7R$^+$ TIs, or DP^{hi} TCR^{med}c-Kit$^-$IL-7R$^+$ cells (Fig. 1), indicating the requirement of positive selection signals (by recognition of self-MHC) for thymocytes to express c-Kit and/or IL-7R on either pathway.

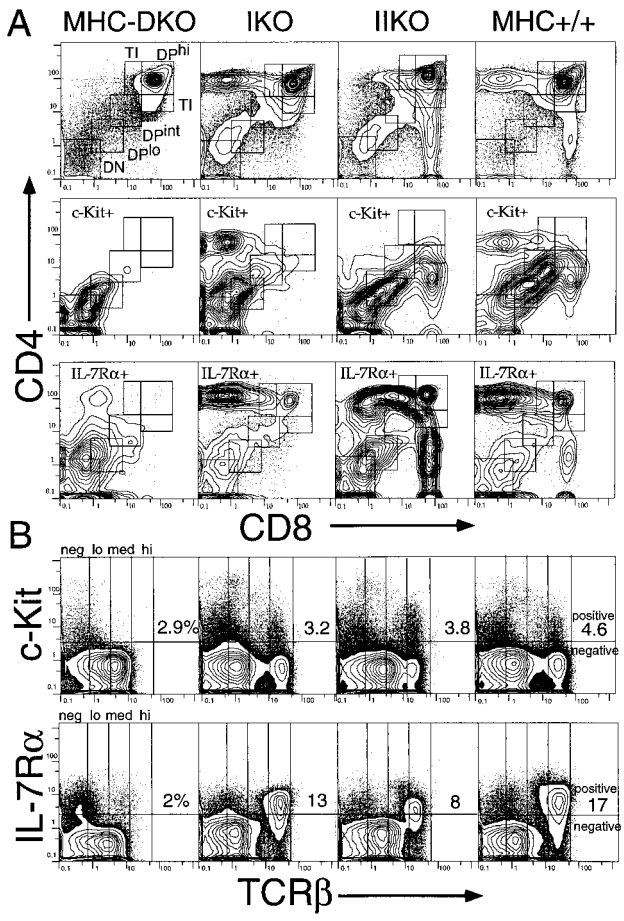

FIG. 1. Distribution of c-Kit$^+$ or IL-7Rα$^+$ cells in either MHC-DKO, MHC-IKO, MHC-IIKO, or MHC$^{+/+}$ thymus. (*A*) The CD4/CD8 profiles of total thymocytes (*Top*), those of c-Kit$^+$ cells (*Middle*), and those of IL-7Rα$^+$ cells (*Bottom*). Squares indicate the definition of DN, DP^{lo}, DP^{int}, DP^{hi}, and TI (CD4$^+$CD8^{med} or CD4^{med}CD8$^+$) stages in this study. (*B*) The TCRβ/c-Kit (*Upper*) and the TCRβ/IL-7R (*Lower*) profiles of total thymocytes. Note that MHC-DKO mice lack the TCR$^{med\text{-}hi}$ c-Kit$^+$ and TCR$^{med\text{-}hi}$ IL-7R$^+$ populations.

DP^{int}TCR^{lo}c-Kit$^+$ IL-7R$^+$ cells are present in MHC-IKO and MHC-IIKO mice (Fig. 2), but within the TCR^{med}c-Kit$^+$ TIs (mostly IL-7R$^+$), CD4$^+$CD8^{med}, but not CD4^{med}CD8$^+$, cells are present in MHC-IKO, whereas CD4^{med}CD8$^+$, but not CD4$^+$CD8^{med}, cells are present in MHC-IIKO mice (Figs. 1 and 2, Table 1). These patterns of distribution of c-Kit$^+$ cells are compatible with our previous data that the CD4$^+$CD8^{med} c-Kit$^+$ and CD4^{med}CD8$^+$c-Kit$^+$ TIs are CD4 and CD8 lineage committed, respectively (6).

Both MHC-IKO and MCH-IIKO mice have ≈0.2% DP^{hi} TCR^{med}c-Kit$^-$IL-7R$^+$ cells (Fig. 1*A*, Table 1). MHC-IKO mice lack CD4^{med}CD8$^+$TCR^{med}c-Kit$^-$IL-7R$^+$ TIs, whereas MHC-IIKO mice possess both CD4$^+$CD8^{med} TCR^{med}c-Kit$^-$IL-7R$^+$ and CD4^{med}CD8$^+$TCR^{med}c-Kit$^-$IL-7R$^+$ TIs, and most of these TCR^{med}c-Kit$^-$IL-7R$^+$ TIs are CD69$^+$ (data not shown). The CD4$^+$CD8^{med} c-Kit$^-$IL-7R$^+$ cells in MHC-IIKO mice corresponds to the CD4$^+$CD8^{med} "co-receptor skewed" cells that have been reported to contain transitional progenitors of CD8 SP cells (14–16).

Differentiation of Thymocytes from MHC-DKO Mice in the Presence of MHC. We expected that the thymuses of MHC-DKO mice contained early progenitors as well as a new class of cells that failed positive selection because no MHC was present. To test for the presence of both types of cells, we injected the whole thymocyte population from MHC-DKO Ly 5.2 mice i.t. to normal congenic C57BL6 Ly 5.1 mice. The time required for the appearance of CD4 and CD8 SP progeny was different. The first peak of CD4 SP progeny appeared at day 3, fell on day 4, increased after day 5, and reached its second peak on day 7 (Fig. 3*A* and 4*A*). However, CD8 SP progeny did not appear until days 4–5, and gradually increased in number until day 7.

TCR$^+$c-Kit$^+$ cells on the c-Kit$^+$ pathway derived from the whole thymocyte population after i.t. injection are shown in Fig. 4*B*. Fig. 3*B* shows serial changes in the number of cells in the TCR$^{lo\text{-}med}$c-Kit$^+$ and TCR^{hi}c-Kit$^+$ populations in the same study. The peak of TCR^{lo}c-Kit$^+$ (DP^{int}) and c-Kit$^+$TCR^{med} (TI) cells could be seen at day 3. The peak of the TCR^{hi}c-Kit$^+$ (TI) cells was seen at day 5, suggesting that the transition from the TCR^{lo}c-Kit$^+$ and TCR^{med}c-Kit$^+$ stages to TCR^{hi}c-Kit$^+$ cells could occur over ≈2 days. Accordingly, the peak for both CD4 and CD8 SP progeny at day 7 could be interpreted as maturation through the c-Kit$^+$ pathway from day 3 TCR^{lo}c-Kit$^+$ (DP^{int}) cells that were differentiated from TCR$^-$c-Kit$^+$ (DN/DP^{lo}) cells. In contrast, the day 3 CD4 SP progeny may be derived from TCR$^{lo\text{-}med}$c-Kit$^-$ (DP^{hi}) cells on the c-Kit$^-$ pathway.

We then tested the differentiation kinetics and outcomes of sorted DP^{hi} TCR$^{lo\text{-}med}$ c-Kit$^-$ and DN/DP^{lo} TCR$^-$c-Kit$^+$ precursors from MHC-DKO mice (Fig. 5). The DP^{hi} TCR$^{lo\text{-}med}$ (c-Kit$^-$ IL-7R$^-$) cells in MHC-DKO mice differentiated almost exclusively to TCR^{hi}CD4 SP cells on day 3 postinjection (Figs. 3*C* and 4). During this transition, c-Kit was not up-regulated (Fig. 4*B*). A very low level of differentiation into CD8 SP cells could be seen on day 6 (Fig. 4*A*). The ratio of CD4 to CD8 progeny was ≈15 to 1 at their peaks (Fig. 3*C*). This preferential differentiation of DP^{hi}c-Kit$^-$ cells to CD4 SP cells also was seen in normal mice (6), although the frequency of progeny in MHC-DKO thymus was ≈3- to 4-fold higher compared with that from normal thymus (see below).

Next, we injected sorted DN/DP^{lo}TCR$^-$c-Kit$^+$ cells (Fig. 5*B*) from DKO thymus. As one might expect from injecting these more primitive progenitors, the SP progeny gradually built up after day 4, and reached their peak at day 7 (Fig. 3*D*).

Table 1. Frequency of TCR^{med} subpopulations in normal and MHC-deficient thymuses

	$TCR^{med}CD4^{hi}CD8^{med}$					$TCR^{med}CD4^{med}CD8^{hi}$					$TCR^{med}DP^{hi}$				
Mice	K^+7R^+	K^+7R^-	K^-7R^+	K^-7R^-	Total	K^+7R^+	K^+7R^-	K^-7R^+	K^-7R^-	Total	K^+7R^+	K^+7R^-	K^-7R^+	K^-7R^-	Total
N	0.06	0.02	0.32	0.46	0.86	0.04	n.d.	0.11	0.42	0.45	n.d.	n.d.	0.18	3.69	3.89
IKO	0.05	0.02	0.23	0.42	0.72	n.d.	n.d.	n.d.	0.44	0.44	n.d.	n.d.	0.16	5.22	5.38
IIKO	n.d.	n.d.	0.18	0.69	0.87	0.04	0.01	0.16	0.24	0.45	n.d.	n.d.	0.20	14.7	14.90
DKO	n.d.	n.d.	n.d.	0.35	0.35	n.d.	n.d.	n.d.	0.24	0.24	n.d.	n.d.	n.d.	38.4	38.40

N: normal; IKO: MHC-IKO; IIKO; MHC-IIKO; DKO: MHC-I and IIKO; K: c-Kit; 7R: IL-7R.
Data are shown as percent of total thymocytes (mean value of three thymuses in each group); n.d.: not detectable (<0.01%).

The $TCR^{lo\text{-}hi}$c-Kit^+ precursors appeared during this transition (Fig. 4*B*). The ratio of CD4 to CD8 progeny was ≈4 to 1.

Based on these data, DP^{hi}c-Kit^- IL-$7R^-$ cells preferentially differentiate to CD4 SP cells on the c-Kit^- pathway, whereas the DN/$DP^{lo}TCR^-$c-Kit^+ cells could generate both CD4 and CD8 progeny. The second peak (day 7) of CD4 progeny could be ascribed partially to the c-Kit^- pathway as well as to the c-Kit^+ pathway. Most injected $DP^{int}TCR^{lo}$c-Kit^+ cells likely failed to receive positive selection because of their expression of inappropriate TCR (for self-MHC) or of a failure in reaching suitable microenvironment; some of these can be selected at the $DP^{hi}TCR^{lo}$c-Kit^- stage on the c-Kit^- pathway.

Cell Cycle Status During Positive Selection on the c-Kit^+ and c-Kit^- Maturation Pathway. The cell cycle status of thymocytes during positive selection was analyzed by dilution of PKH26 labeling of injected cells. Each doubling of labeled cells corresponds to a 50% drop of the mean fluorescent signal (8).

As shown in Fig. 6, both the $TCR^{-/lo}$c-Kit^+ and the TCR^{med}c-Kit^+ populations showed a similar declining pattern of the PKH26 signal after i.t. injection. Because the $TCR^{-/lo}$c-Kit^+ cells proliferate and differentiate without major input from more primitive intrathymic populations, the decline in PKH26 levels in cells retaining this phenotype reflects self-renewing divisions. The estimated cell cycle time for these cells was 10.8 hr. The appearance of the TCR^{hi}c-Kit^+ population that possessed the same declining intensity of PKH26 signals was delayed by ≈2 days. This finding indicates that it takes ≈2 days for TCR^{med}c-Kit^+ cells to reach the TCR^{hi}c-Kit^+ stage. Similarly, the interval between the transition from the TCR^{hi}c-Kit^+ to the TCR^{hi}c-Kit^- stage could be estimated as ≈1 day; TCR^{hi}c-Kit^- CD8 SP cells on the first evaluable day (day 5) should be derived mainly from the c-Kit^+ pathway, and the mean PKH level in the day 5 TCR^{hi}c-Kit^- CD8 SP cells almost corresponded to that of day 4 TCR^{hi}c-Kit^+ cells. The slower decline of PKH levels in the TCR^{hi}c-Kit^- CD8 SP cells compared with those of c-Kit^+ compartments might indicate the accumulation of positively selected cells at this stage (17).

The PKH26 intensity of each CD4/CD8-defined progeny derived from the total MHC-DKO thymus is shown in Fig. 7*A*. The CD4 SP and DP cells on day 3 retain almost the same intensity as the injected cells. The day 5 CD4 SP progeny retain PKH26 at levels consistent with 0–2 cell divisions, whereas the day 7 CD4 SP progeny included populations that had undergone several cell divisions. On the other hand, all CD8 SP progeny observed on or after day 5 postinjection showed a significant decline of PKH26 signals, indicating several cell divisions of their progenitors.

The PKH26-labeled DP^{hi}c-Kit^- cells from MHC-DKO mice differentiated into CD4 SP cells without cell division (0.05 cell cycles), as we reported (8), whereas in normal mice, more than 60% of the day 3 CD4 SP progeny of DP^{hi}c-Kit^- cells from normal mice had undergone cell division (1.2 times on average) (Fig. 7*B*). In contrast to the days 5 and 7 CD8 progeny from unseparated MHC-DKO thymocytes, the rare day 7 CD8 SP progeny from MHC-DKO DP^{hi}c-Kit^- cells had divided 0–2 times (1.1 times on average) (Fig. 7*B*).

DP c-Kit^- Thymocytes in MHC-DKO Mice Contain Higher Percentages of Selectable Cells that Express Multiple TCRα Chains. We evaluated the numbers of progenitors in DP^{hi}c-Kit^- cells in normal and MHC-DKO thymuses 3 and 4 days after i.t. injection. As shown in Fig. 8*A*, the DP^{hi}c-Kit^- cells in MHC-DKO mice contained ≈3- to 4-fold higher numbers of progenitors compared with those in normal mice. This finding suggests that the DP^{hi}c-Kit^- cells in MHC-DKO mice could contain a higher percentage of cells expressing self-MHC selectable TCRα/β, both by their default transition to DP^{hi} in MHC-DKO thymuses as well as by new TCRα chain expres-

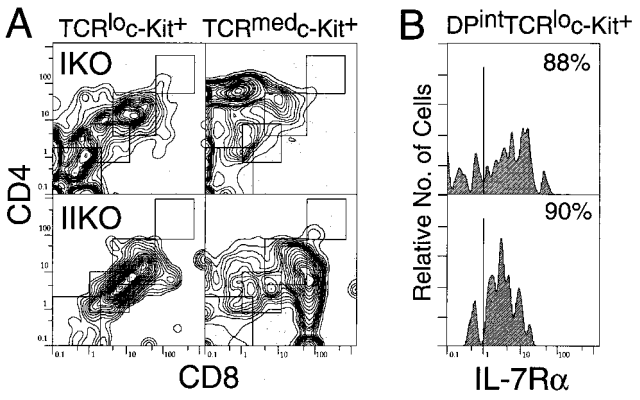

FIG. 2. (*A*) CD4/CD8 profiles of $TCR^{lo\text{-}med}$c-Kit^+ cells in either MHC-IKO or IIKO mice. The TCR^{lo}c-Kit^+ cells contains DP^{int} cells. In TCR^{med}c-Kit^+ population, MHC-IKO mice lack $CD4^{med}CD8^+$ TIs, whereas MHC-IIKO mice lack $CD4^+CD8^{med}$ TIs. (*B*) The $DP^{int}TCR^{lo}$c-Kit^+ cells express IL-7R in both MHC-IKO and IIKO mice.

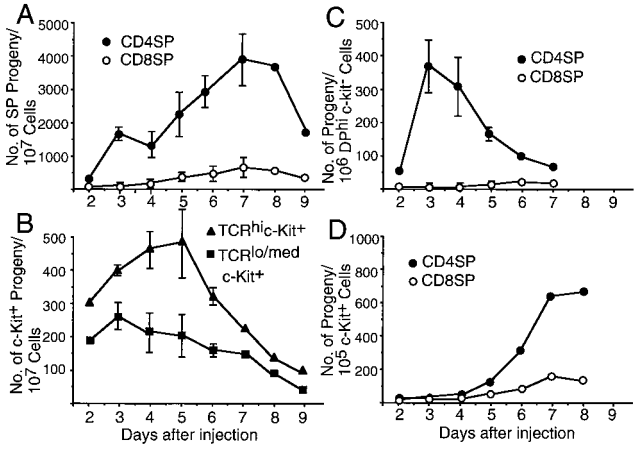

FIG. 3. Changes in number of progeny after i.t. injection of various thymocyte populations from MHC-DKO mice into $MHC^{+/+}$ hosts. (*A*) CD4 and CD8 SP progeny from unfractionated thymocytes. (*B*) TCRβ/c-Kit-defined progeny from unfractionated thymocytes. (*C*) CD4 and CD8 SP progeny from DP^{hi} ($TCR^{lo\text{-}med}$) c-Kit^- thymocytes. (*D*) CD4 and CD8 SP progeny from TCR^-c-Kit^+ thymocytes. Data are shown as mean values more than two independent experiments. Error bars indicate standard deviations.

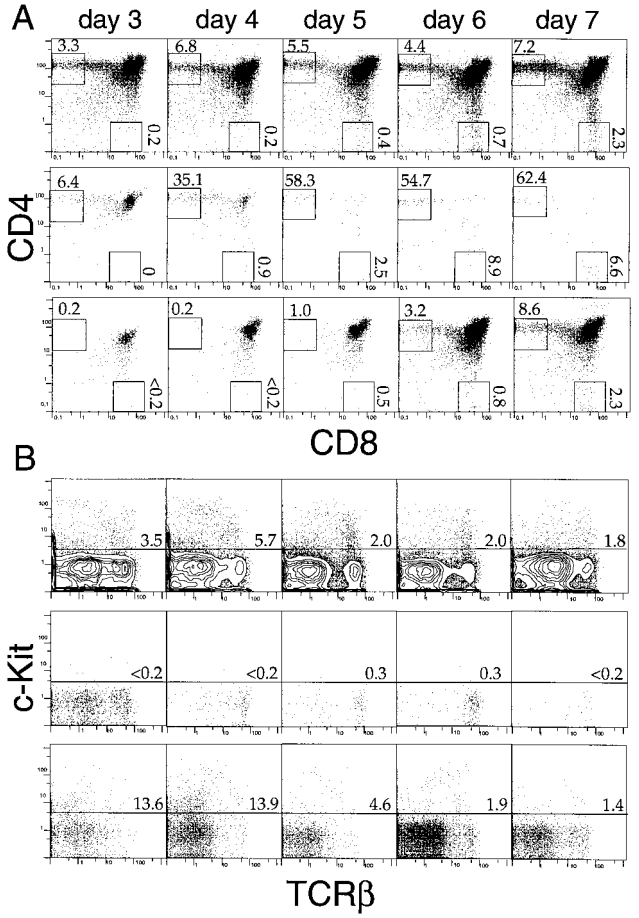

FIG. 4. *In vivo* differentiation of MHC-DKO thymocytes after i.t. injection into MHC$^{+/+}$ hosts. (*A*) CD4/CD8 profiles of progeny from unfractionated (*Top*), sorted DP^{hi}c-Kit^{-} (*Middle*), and DN/DP^{lo}c-Kit^{+} thymocytes (*Bottom*) from MHC-DKO mice after i.t. injection. (*B*) TCRβ/c-Kit profiles of progeny from unfractionated (*Top*), sorted DP^{hi}c-Kit^{-} (*Middle*), and DN/DP^{lo}c-Kit^{+} thymocytes (*Bottom*) from MHC-DKO mice after i.t. injection. Numbers indicate percentages of gated fractions.

sion (10, 11). Fig. 8*B* shows the Vα2/Vα3 and Vα2/Vα8.2 profiles of TCR$^{lo\text{-}med}$c-Kit^{-} cells in MHC-DKO and MHC-positive (class I$^{+/-}$ and II$^{+/-}$) (MHC$^{+/-}$) mice. As predicted, the MHC-DKO mice contain ≈5- to 6-fold higher numbers of TCR$^{lo\text{-}med}$c-Kit^{-} (DP^{hi}) TCRVα-double-expressing cells compared with MHC$^{+/-}$ mice.

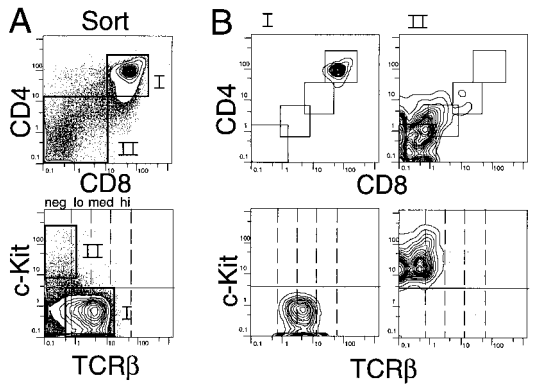

FIG. 5. Gates for sorting (*A*) and phenotypes of sorted populations on reanalysis (*B*) for DP^{hi}TCR$^{lo\text{-}med}$c-Kit^{-} (I) and DN/DP^{lo}TCR^{-}c-Kit^{+} (II) populations from MHC-DKO thymus. Resorted cells were injected into MHC$^{+/+}$ thymus.

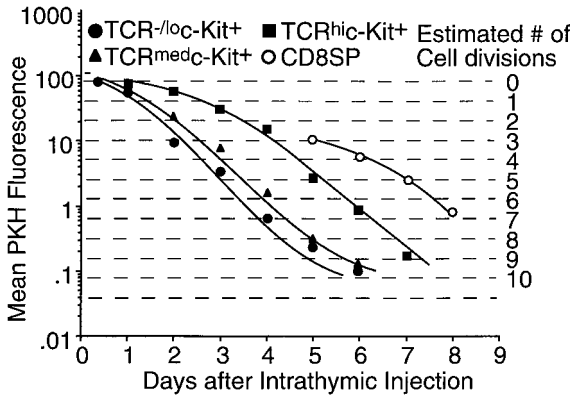

FIG. 6. Changes of PKH26 signal intensity in TCR/c-Kit-defined subsets from MHC-DKO mice after i.t. injection to MHC$^{+/+}$ hosts. The estimated numbers of cell divisions are shown as broken lines. Each dot stands for the mean signal intensity of each population. There was a wide variation of PKH26 intensities in each subset.

Blockade of IL-7R and c-Kit Signaling by Neutralizing Anti-IL-7Rα and Anti-c-Kit Antibodies Prevent Positive Selection on the c-Kit^{+} Maturation Pathway. Most TCR$^{lo\text{-}med}$c-Kit^{+} cells also express IL-7R and rapidly proliferate during positive selection *in vivo*. To clarify the role of signals from these cytokine receptors on positive selection *in vivo*, we evaluated the effect of neutralizing anti-IL-7Rα (A7R34) and anti-c-Kit (ACK2) antibodies on the c-Kit^{+} maturation pathway in normal mice. As shown in Fig. 9, A7R34 and/or ACK2 significantly eliminate each TCR$^{lo\text{-}hi}$ c-Kit^{+} compartment within 3 days.

DISCUSSION

In this paper, we delineated events in the process of thymocyte positive selection on two identifiable pathways; the c-Kit^{+} (IL-7R^{+}) pathway and the c-Kit^{-} (IL-7R^{+}) pathway. We propose that the c-Kit^{-} pathway may be a salvage pathway for cells that had once failed to receive positive selection on the c-Kit^{+} pathway. Fig. 10 represents a composite model of the events described in the discussion.

The majority of DN-DP^{lo}TCR^{-}c-Kit^{+}IL-7R^{+} cells in MHC-DKO mice are more mature precursors compared with the earliest thymic precursors (1), because they have rearranged their TCRβ chains (data not shown), and they generated SP

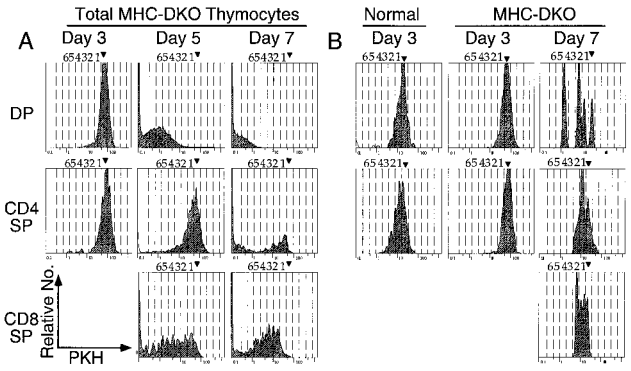

FIG. 7. The PKH26 profile in CD4 SP and CD8 SP progeny after i.t. injection. (*A*) Serial changes of PKH26 profiles after i.t. injection of PKH26-stained total thymocytes from MHC-DKO mice. (*B*) Serial changes of PKH26 profiles after i.t. injection of PKH26-stained DP^{hi}c-Kit^{-} (TCR$^{lo\text{-}med}$) thymocytes from MHC-DKO mice and normal mice. Vertical broken lines correspond to the 50% decrease of fluorescence intensity of PKH26. The numbers above each panel depict the estimated numbers of cell divisions as determined by the decline of PKH26 intensity.

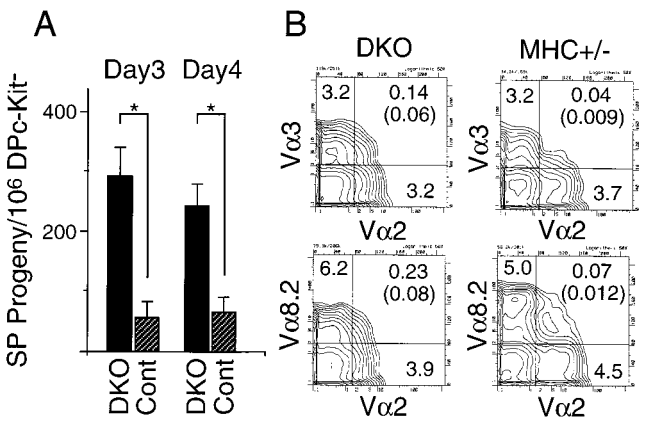

FIG. 8. (*A*) The absolute numbers of days 3 and 4 CD4 SP progeny from 2×10^6 $DP^{hi}c\text{-}Kit^-$ cells from MHC-DKO and $MHC^{+/+}$ (Cont) mice. *, $P < 0.05$. (*B*) TCR Vα2/Vα3 and TCR Vα2/Vα8.2 profiles of gated $TCR\beta^{lo\text{-}med}$ thymocytes in MHC-DKO and $MHC^{+/-}$ mice. The numbers show the percentages of each subpopulation, and numbers in parenthesis indicate the percentage in total thymocytes. MHC-DKO thymocytes contain ≈6-fold more $TCR^{lo\text{-}med}$ cells that coexpress two different TCRα chains than in $MHC^{+/-}$ mouse thymus. Data are shown on two-parameter logarithmic plots (50%).

progeny as short as 5–7 days after i.t. injection. MHC-DKO mice lack populations on the $c\text{-}Kit^+$ maturation pathway beyond the DN/DP^{lo} early progenitors except for small numbers of $DP^{int}TCR^{lo}c\text{-}Kit^+IL\text{-}7R^+$ cells. This finding suggests that most $DP^{int}TCR^{lo}c\text{-}Kit^+IL\text{-}7R^+$ cells in normal mice might be in the process of being positively selected, though these cells have not shown the I-A allele-specific positive selection (and enrichment) of Vβ17a TCR^+ cells (6). It took ≈3 days for the $TCR^-c\text{-}Kit^+$ cells to expand and become $TCR^{lo\text{-}med}c\text{-}Kit^+$ cells (Fig. 3*B*); this might cause ≈3 days' delay of significant production of SP progeny on the $c\text{-}Kit^+$ pathway compared with that on the $c\text{-}Kit^-$ pathway, because in normal mice, $TCR^{lo}c\text{-}Kit^+$ cells could generate SP cells ≈4 days after i.t. injection (6). The possible role of pre-TCRα/TCRβ receptor complex (18) on the proliferation of cells during the transition from $DN/DP^{lo}TCR^-c\text{-}Kit^+IL\text{-}7R^+$ to $DP^{int}TCR^{lo}c\text{-}Kit^+IL\text{-}7R^+$ stages remains unclear. The transition from cycling $TCR^{med}c\text{-}Kit^+$ ($IL\text{-}7R^+$) to noncycling $TCR^{hi}c\text{-}Kit^+(IL\text{-}7R^+)$ TIs, and from $TCR^{hi}c\text{-}Kit^+$ ($IL\text{-}7R^+$) TIs to $TCR^{hi}c\text{-}Kit^-$ ($IL\text{-}7R^+$) SP cells could be estimated as ≈2 and ≈1 days,

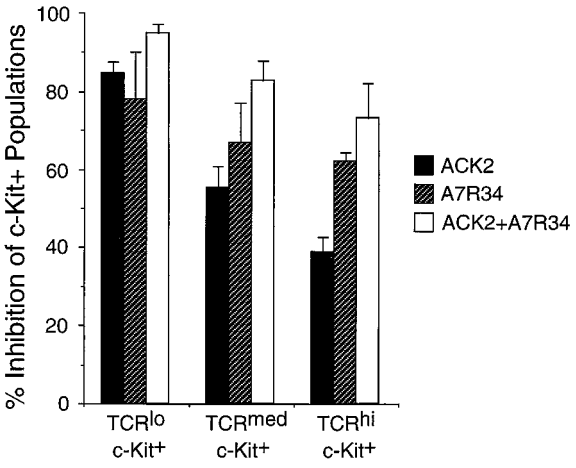

FIG. 9. The effects of neutralizing anti-c-Kit (ACK-2) and anti-IL-7Rα (A7R34) antibodies on the $c\text{-}Kit^+$ pathway in normal mice. One milligram of these antibodies was i.p. injected, and thymocytes were analyzed on day 3 postinjection by using anti-c-Kit (2B8) antibody.

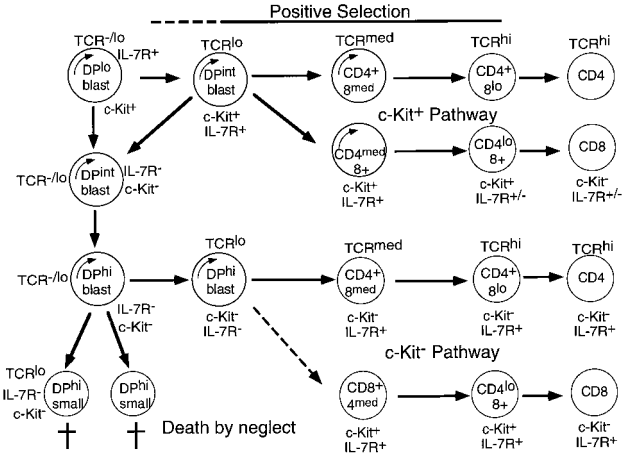

FIG. 10. A model of thymic differentiation. In this model, DP^{int} $TCR^{lo}c\text{-}Kit^+$ cells begin the process of self-MHC recognition; successful recognition propels these cells along $c\text{-}Kit^+$ maturation path to CD4 and CD8 SP cells maintaining IL-7R and Bcl-2 (6) (along the lines depicted on the top). Curved arrows indicate cells in the mitotic cycle. $DP^{int}TCR^{lo}c\text{-}Kit^+$ cells that fail positive selection (and also $DP^{lo}TCR^{-/lo}$ blasts) can enter the $c\text{-}Kit^-$ pathway by down-regulating c-Kit, IL-7R, and Bcl-2, and up-regulating CD4 and CD8 to become DP^{hi} blast cells. Within the $DP^{hi}TCR^{lo}c\text{-}Kit^-$ blast cell population, alternative TCRα rearrangement can occur. The majority of such cells again fail positive selection, become small $DP^{hi}TCR^{lo}c\text{-}Kit^-IL\text{-}7R^-$ ($Bcl\text{-}2^-$) cells that die by neglect (6). A subset of $DP^{hi}TCR^{lo}c\text{-}Kit^-$ cells that have gained TCRα/β receptor that are self-MHC-restricted enter the $c\text{-}Kit^-IL\text{-}7R^+$ maturation pathway up-regulating Bcl-2 (8), and differentiate mainly to CD4 SP cells (the middle horizontal sequences). IL-7R principally signals survival of cells on both pathways through up-regulating (at least) Bcl-2 (8).

respectively, by the interval between the appearance of peaks and that of cells of the same PKH26 intensity in these compartments.

The estimated doubling time in cycling $TCR^{lo\text{-}med}c\text{-}Kit^+$ ($IL\text{-}7R^+$) cells (≈11 hr) is slightly slower than those in the majority of blast cells (6–9 hr) (19). This expansion of the cycling $c\text{-}Kit^+$ cells might be dependent on both the proliferation-inducing signals from c-Kit (3) and survival-promoting signals from IL-7R (8, 9), because the neutralizing anti-IL-7Rα or anti-c-Kit antibodies could inhibit their proliferation.

The transition from TCR^{hi} $c\text{-}Kit^+$ ($IL\text{-}7R^+$) TIs to TCR^{hi} $c\text{-}Kit^-(IL\text{-}7R^+)$ SP cells, which mainly involves the down-regulation of either coreceptor does not involve proliferation. The MHC-IKO lack the $CD4^{med}CD8^+TCR^{med}c\text{-}Kit^+$ $IL\text{-}7R^+$ TIs and the MHC-IIKO mice lack the $CD4^+CD8^{med}$ $TCR^{med}c\text{-}Kit^+$ $IL\text{-}7R^+$ TIs. We have shown that the $CD4^+CD8^{med}$ $c\text{-}Kit^+$ TIs and the $CD4^{med}CD8^+$ $c\text{-}Kit^+$ TIs differentiated almost exclusively into CD4 and CD8 SP cells *in vitro*, respectively (6). Accordingly, the majority of cells restricted to MHC class I on the $c\text{-}Kit^+$ pathway differentiate into SP cells without passing through the $CD4^+CD8^{lo\text{-}med}$ transition (20–22).

Thymocytes that failed positive selection at the DP^{int} $TCR^{lo}c\text{-}Kit^+$ $IL\text{-}7R^+$ stage down-regulate c-Kit and IL-7R and become DP^{hi} $TCR^{lo}c\text{-}Kit^-$ $IL\text{-}7R^-$ cells (6). In MHC-DKO mice, the lack of MHC could cause cells with otherwise appropriate anti-self-MHC restricted TCRs also to undergo default maturation to DP^{hi} cells. These DP^{hi} $c\text{-}Kit^-$ $IL\text{-}7R^-$ cells can express two TCRα chains (Fig. 8) (10, 11) These DP^{hi} blast cells from MHC-DKO mice therefore contain increased numbers of cells capable of receiving positive selection, although they are less efficient on a per-cell basis than $DP^{int}c\text{-}Kit^+$ cells (6). DP^{hi} blast cells on the $c\text{-}Kit^-$ pathway begin to express IL-7R, and the signaling through the receptor promotes survival of positively selected cells (8). The $DP^{hi}c\text{-}Kit^-$ cells undergo mainly CD4 lineage maturation for the first 4

days, and a small number of CD8 SP progeny could be detected on days 5–7 postinjection. It has been reported that a $CD4^+$ $CD8^{lo\text{-}med}$ TIs can give rise to some CD8 SP cells (16, 20–22). It is possible that a fraction of CD8 SP progeny derived late from DP^{hi}c-Kit^- cells might go through the transitional stage of $CD4^+CD8^{med}$c-Kit^-IL-$7R^+$ cells; the $CD4^+CD8^{lo\text{-}med}$ c-Kit^- IL-$7R^+$ cells in the MHC-IIKO mice could differentiate into CD8 SP cells 3–4 days after i.t. injection into congenic normal mice (unpublished data).

These results do not address patterns of development of cells expressing known TCR$\alpha\beta$ with known MHC-peptide specificity; the study of thymic positive selection in TCR transgenic mice addresses the issue of specificity, but because in these mice TCR expression is not appropriately regulated (from TCR^{lo} to TCR^{hi}), DP cells in TCR transgenic mice contain a considerable fraction of small to medium-sized $TCR^{med\text{-}hi}$ cells (23–25). Although we do not detect measurable positive selection of nonblastic DP cells in our studies (4), other studies using small DP^{hi} cells from TCR transgenic mice can differentiate into SP cells (26) without cell division, as shown in a bromodeoxyuridine labeling study (27).

Several studies on continuous labeling with bromodeoxyuridine or tritiated thymidine (^{3}H-TdR) suggests that positive selection does not involve cell division, because of a 2–3 days' lag in the entry of labeled cells into the SP cell fraction (28, 29). However, the lag could be ascribed to the time required for completing the noncycling late stage of positive selection that involves down-regulation of unused coreceptor and final up-regulation of TCR. In contrast, in this study and in our previous study (6), considerable cell proliferation contributes to positive selection on the c-Kit^+ pathway.

This study also suggests potential biological differences in positive selection between CD4 and CD8 lineage maturation. Other receptor-mediated signals such as Notch might affect the lineage outcomes of DP cells (30), and that may result in the strong bias to CD4 lineage differentiation from DP^{hi}c-Kit^- cells. Hunig and Mitnacht (31) have reported rapid and prominent generation of mature CD8 SP cells from TCR-stimulated virgin DP cells *in vitro*. How this finding compares with intrathymic maturation pathways described here is unclear; this rapid process cannot be explained by the CD8 maturation scheme that involves complex CD4 down-regulation (16, 21).

Thus, we have demonstrated two positive selection pathways, which probably represent sequential events. In this view, the first pathway that is attempted is the c-Kit^+IL-$7R^+$ one, to be followed by the c-Kit^-IL-$7R^+$ path in cells that have failed a first round of positive selection with a particular TCRα/β. It is also possible that they can represent two independent pathways, in which case, there is a considerable diversity in positive selection.

We are indebted to Dr. S. Nishikawa for A7R34 and ACK2 and Drs. M. J. Grusby and L. H. Glimcher for $MHC^{-/-}$ mice. This work was mainly supported by U.S. Public Health Service Grant CA-42551.

1. Wu, L., Scollay, R., Egerton, M., Pearse, M., Spangrude, G. J. & Shortman, K. (1991) *Nature (London)* **349,** 71–74.
2. Godfrey, D. I., Kennedy, J., Suda, T. & Zlotnik, A. (1993) *J. Immunol.* **150,** 4244–4252.
3. Rodewald, H.-R., Kretzschmar, K., Swat, W. & Takeda, S. (1995) *Immunity* **3,** 313–319.
4. Guidos, C. J., Danska, J. S., Fathman, C. G. & Weissman, I. L. (1990) *J. Exp. Med.* **172,** 835–845.
5. Shortman, K., Vremec, D. & Egerton, M. (1991) *J. Exp. Med.* **173,** 323–332.
6. Akashi, K. & Weissman, I. L. (1996) *Immunity* **5,** 147–161.
7. Sudo, T., Nishikawa, S., Ohno, N., Akiyama, N., Tamakoshi, M., Yoshida, H. & Nishikawa, S.-I. (1993) *Proc. Natl. Acad. Sci. USA* **90,** 9125–9129.
8. Akashi, K., Kondo, M., von Freeden-Jeffry, U., Murray, R. & Weissman, I. L. (1997) *Cell* **89,** 1033–1041.
9. Kondo, M., Akashi, K., Domen, J., Sugamura, K. & Weissman, I. L. (1997) *Immunity* **7,** 155–162.
10. Borgulya, P., Kishi, H., Uematsu, Y. & von Boehmer, H. (1992) *Cell* **69,** 529–537.
11. Petrie, H. T., Livak, F., Schatz, D. G., Strasser, A., Crispe, I. N. & Shortman, K. (1993) *J. Exp. Med.* **178,** 615–622.
12. Grusby, M. J., Auchincloss, H., Jr., Lee, R., Johnson, R. S., Spencer, J. P., Zijlstra, M., Jaenisch, R., Papaioannou, V. E. & Glimcher, L. H. (1993) *Proc. Natl. Acad. Sci. USA* **90,** 3913–3919.
13. Kondo, M., Ohashi, Y., Tada, K., Nakamura, M. & Sugamura, K. (1994) *Eur. J. Immunol.* **24,** 2026–2030.
14. van Meerwijk, J. P. M. & Germain, R. N. (1993) *Science* **261,** 911–915.
15. Lucas, B., Vasseur, F. & Penit, C. (1995) *J. Exp. Med.* **181,** 1623–1633.
16. Lucas, B. & Germain, R. N. (1996) *Immunity* **5,** 461–477.
17. Scollay, R. & Godfrey, D. I. (1995) *Immunol. Today* **16,** 268–273.
18. Groettrup, M., Ungewiss, K., Azogui, O., Palacios, R., Owen, M. J., Hayday, A. C. & von Boehmer, H. (1993) *Cell* **75,** 283–294.
19. Metcalf, D. & Wiadrowski, M. (1966) *Cancer Res.* **26,** 483–489.
20. Lundberg, K., Heath, W., Kontgen, F., Carbone, F. R. & Shortman, K. (1995) *J. Exp. Med.* **181,** 1643–1651.
21. Kydd, R., Lundberg, K., Vremic, D., Harris, A. W. & Shortman, K. (1995) *J. Immunol.* **155,** 3806–3814.
22. Suzuki, H., Punt, J. A., Granger, L. G. & Singer, A. (1995) *Immunity* **2,** 413–425.
23. Ohashi, P. S., Pircher, H., Burki, K., Zinkernagel, R. M. & Hengartner, H. (1990) *Nature (London)* **346,** 861–863.
24. Borgulya, P., Kishi, H., Muller, U., Kirberg, J. & von Boehmer, H. (1991) *EMBO J.* **10,** 913–918.
25. Swat, W., Dessing, M., Baron, A., Kisielow, P. & von Boehmer H. (1992) *Eur. J. Immunol.* **22,** 2367–2372.
26. Lundberg, K. & Shortman, K. (1994) *J. Exp. Med.* **179,** 1475–1483.
27. Huesmann, M., Scott, B., Kisielow, P. & von Boehmer, H. (1991) *Cell* **66,** 533–540.
28. Penit, C. (1986) *J. Immunol.* **137,** 2115–2121.
29. Egerton, M., Scollay, R. & Shortman, K. (1990) *Proc. Natl. Acad. Sci. USA* **87,** 2579–2582.
30. Robey, E., Chang, D., Itano, A., Cado, D., Alexander, H., Lans, D., Weinmaster, G. & Salmon, P. (1996) *Cell* **87,** 483–492.
31. Hunig, T. & Mitnacht, R. (1991) *J. Exp. Med.* **173,** 561–568.